RESEARCH ARTICLES

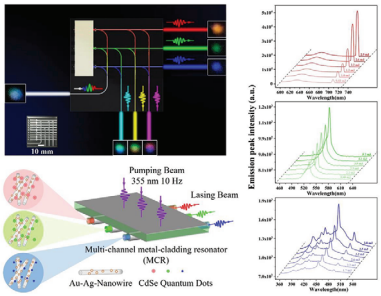

This research introduces a novel multicolor microlaser that integrates semiconductor quantum dots, a multichannel metal-cladding resonator (MCR), and Au-Ag nanowires. Achieving low-threshold, multicolor, and directional output lasing from CdSe quantum dots, the system utilizes the MCR for enhanced power density and Au-Ag nanowires for improved scattering feedback. The proposed micro-laser holds promise for applications in active photonic chips.

ADVANCED OPTICAL MATERIALS
www.advopticalmat.de

Miniaturization of Multicolor Quantum Dots Lasing Based on 2D Constrained Resonator

Meng Zhang, Hailang Dai, Yanbo Zhao, and Xianfeng Chen**

Elevated expectations for laser performance, encompassing broadband tunability, integration, low power consumption, and a low threshold, have emerged within the realms of photonic chips and optoelectronic devices. Nevertheless, achieving multicolor miniaturized lasers within a singular micro-nano structure remains challenging, hindered by constraints in geometric structure, optical gain, and bandgap considerations. Here, an approach to obtain integrated multicolor lasing beam output simultaneously in a desired direction from a 2D-constrained micro-resonator is proposed. The wavelength of the lasing beam is tuned by controlling the size of quantum dots (QDs) in the resonator. Owing to the high density of power within the cavity and the localized surface plasmon resonance on the surface of the Au-Ag nanowires (NWs), a notably low laser threshold is realized in the micro-resonator channel. This work introduces a method for realizing an integrated multicolor micro-laser, providing a pathway toward the implementation of active photonic chips and advanced optoelectronic devices.

1. Introduction

Multicolor or multiwavelength lasers, covering a broad spectral range have applications in color laser display, chemical and biological sensing, as well as photonic computers and on-chip optical communications.[1–5] While the characteristics and demands of lasers vary across different domains, the imperative for multiwavelength, tunable miniaturization persists in the realm of integrated photonic chips and optoelectronic devices.[6–9] One approach involves the subtle tuning of the micro-laser wavelength by modifying the dielectric environment of the cavity. This adjustment can be achieved through variations in excitation intensity, sample temperature, surface plasma polaritons, cavity design, or substrate properties.[10–15] However, this approach is constrained by a limited wavelength range, as the free spectral range typically falls short of the full width at half maximum of the gain curve. Another approach involves controlling the emission wavelength by tuning the composition of the gain medium, offering a significantly larger wavelength tuning range. Examples include semiconductor quantum dots (QDs) lasers and nanowires (NWs) lasers.[16–20] Therein, a variety of multicolor micro-nano scale lasers have been accomplished through the utilization of low-dimensional semiconductor structures with an adjustable bandgap.[21] Based on reported findings on QDs and NWs lasers, the majority exhibit overlapping and blended lasing beams lacking directionality and featuring low intensity. This makes their practical integration into photonic chips and optoelectronic devices challenging. Although considerable efforts have been invested in achieving multiwavelength tunable miniaturization of lasers, obtaining multicolor miniaturization within a single micro-nano structure remains difficult due to stringent requirements for regular geometric structure, high optical gain, and a bandgap-graded profile.

To overcome these challenges, we propose an approach to achieve the output of multicolor lasing beams in a desired direction from a single chip utilizing a 2D-constrained micro-resonator. This micro-resonator comprises Au nanoparticles (Au NPs), Ag nanowires (Ag NWs), and a multichannel metal-cladding resonator (MCR). The Au NPs grow on the Ag nanowire surface via a chemical reaction, enabling the focusing and confinement of the surface plasmonic wave (SPW) within a small volume located between the nanogap of the Au NPs and the surface of the Ag NWs. Therein, the density of the electric field power has been enhanced in the gap. Additionally, owing to the small incident angle, the effective refractive index (N_{eff}) of the MCR ranges between 0 and 1 in each channel.[22] Light can be effectively trapped in the resonator,[23] facilitating comprehensive interaction between light and QDs within the MCR channel. In our study, upon injecting a mixture solution of QDs and Au-Ag NWs into the MCR, we achieved on-chip multicolor lasing with the desired directional output, miniaturization, and low threshold, as illustrated in **Figure 1**. This on-chip multicolor laser has advantages over microdisks, photonic crystals, plasmonic nanostructures, or random lasers in that it can achieve directional laser output, change the types and wavelengths of gain media, and possesses higher efficiency and applicability, as well as lower cost.

M. Zhang, H. Dai, Y. Zhao, X. Chen
State Key Laboratory of Advanced Optical Communication Systems and Networks
School of Physics and Astronomy
Shanghai Jiao Tong University
Shanghai 200240, China
E-mail: hailangdai@sjtu.edu.cn; xfchen@sjtu.edu.cn
X. Chen
Collaborative Innovation Center of Light Manipulations and Applications
Shandong Normal University
Jinan 250358, China

The ORCID identification number(s) for the author(s) of this article can be found under https://doi.org/10.1002/adom.202400017

DOI: 10.1002/adom.202400017

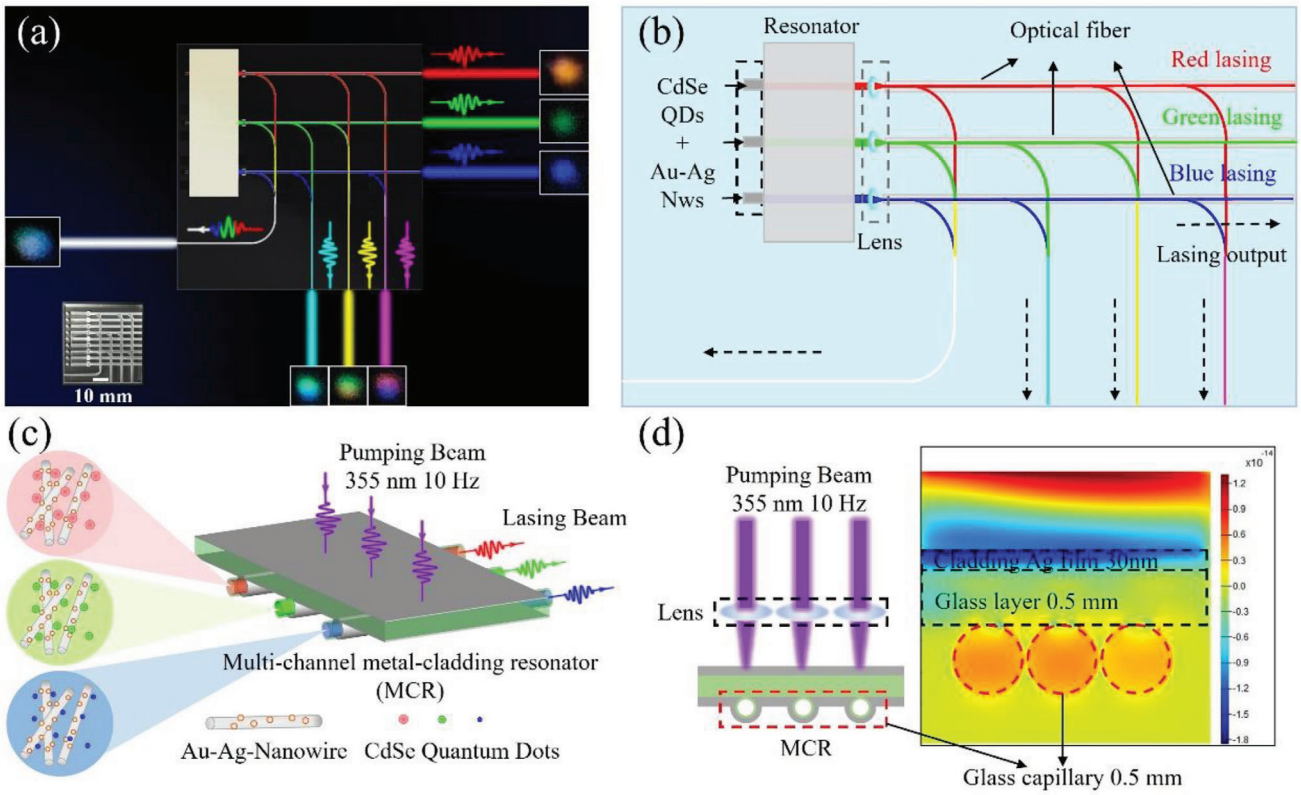

Figure 1. a) Vision of our integrated chip: achieving simultaneous red, green, and blue lasing outputs from the MCR, with each color independently transferred via an optical fiber. The diameter of the optical fiber is 1 mm. Additionally, the Y-style optical fiber allows for the simultaneous mixing to produce cyan, yellow, and purple lasing outputs. Furthermore, the combination of these colors results in a white lasing output through the three-channel optical fiber during the transfer process. Inset: a picture of our multicolor laser chip. b) Schematic of integrated RGB lasing utilizing our chip: CdSe QDs solutions with three luminescent bands are blended with Au-Ag NWs and injected into three channels of the MCR, respectively. Lasing emission is achieved along the capillary using a 355 nm, 10 Hz nanosecond pulse pump, and the generated laser is coupled into the fiber through lens convergence. c) Schematic diagram of MCR laser. d) The distribution of electric field intensity in the MCR at the excitation wavelength of 355 nm.

2. Results and Discussion

As illustrated in Figure 1a, we propose the development of an on-chip integrated multicolor micro-laser utilizing a three-channel MCR. The versatility of the system is demonstrated, as a single channel of MCR excitation produces red, green, and blue three-color lasing port outputs under the exciting pumping light when the CdSe quantum dots (CdSe QDs) solutions of three luminescent bands are blended with Au-Ag NWs and injected, respectively. Moreover, the red, green, and blue three-color lasing from the MCR is directly coupled into the optical fiber by micro-lens for transmission, respectively. To achieve multicolor lasing, the different color lasing beams are combined into a single beam using either a Y-style or a three-channel optical fiber. Therefore, the port outputs of cyan, yellow, and purple lasing beams are a result of the mixing of double-color lasing beams in the Y-style optical fiber during the transfer process, respectively. Additionally, the three-channel optical fiber produces a white lasing output when red, green, and blue lasing are simultaneously excited and mixed. The picture of our multicolor laser chip is inset in Figure 1a. Visual representations of the output laser spots from the optical fiber are depicted in Figure 1a. Each channel of the MCR is a hollow-core capillary that accommodates a mixture of CdSe QDs and Au-Ag nanowires (Au-Ag NWs), as illustrated in Figure 1c. The excitation source is a nanosecond pulsed laser with a wavelength of 355 nm and a repetition rate of 10 Hz. The combination of CdSe QDs and Au-Ag NWs induces stimulated emission within the MCR, resulting in lasing output along the cavity. The emitted lasing is efficiently coupled into the optical fiber through convergence facilitated by a small lens, with a focal length of 1 mm. In Figure 1d, the electric field distribution cases are depicted using the FDTD software to demonstrate the high power density of the field in each hollow-core capillary of the MCR. The simulation reveals a robust electric field within the MCR channel, crucially supporting the stimulated emission of CdSe QDs.

To provide a detailed description of the field in the MCR and understand the mechanism of lasing output, numerical simulations were conducted using COMSOL 6.0 software. In **Figure 2a**, the structural composition of the MCR is delineated, consisting of four layers arranged from top to bottom: a 30 nm thick Ag film serving as the cladding layer, a 0.5 mm thick glass layer functioning as the waveguide, a capillary with an inner diameter of 0.5 mm serving as the cavity channel, and a layer of 300 nm thick Ag film as the substrate layer to prevent mode leakage from the bottom. The synthesis of Ag NWs involved a hydrothermal method, while Au-Ag NWs were obtained through a substitution

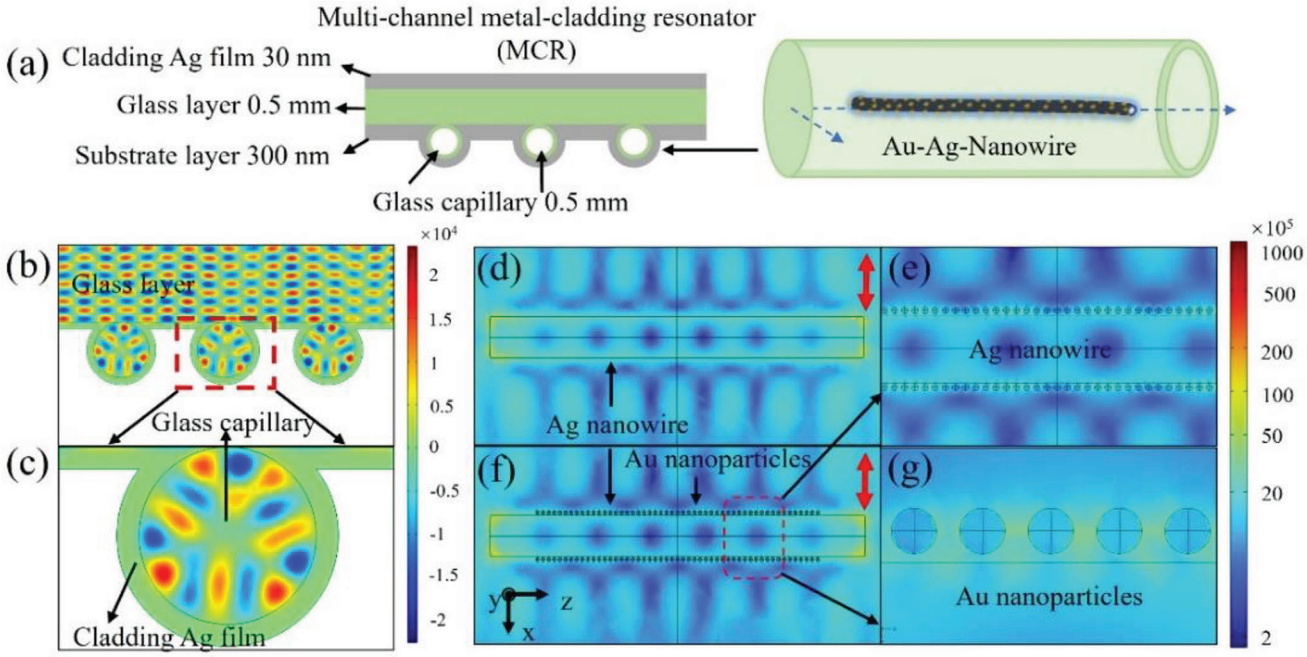

Figure 2. a) Structural diagrams of MCR and Au-Ag NWs. b,c) The electric field intensity distribution in the MCR caused by the incoming field at the excitation wavelength of 355 nm. d–g) The electric field intensity distribution caused by the incoming field near the pure Ag NWs and Au-Ag NWs at the excitation wavelength of 355 nm. The red arrows denote the polarization of the excitation beam. A detailed description is provided in the Supplementary Materials.

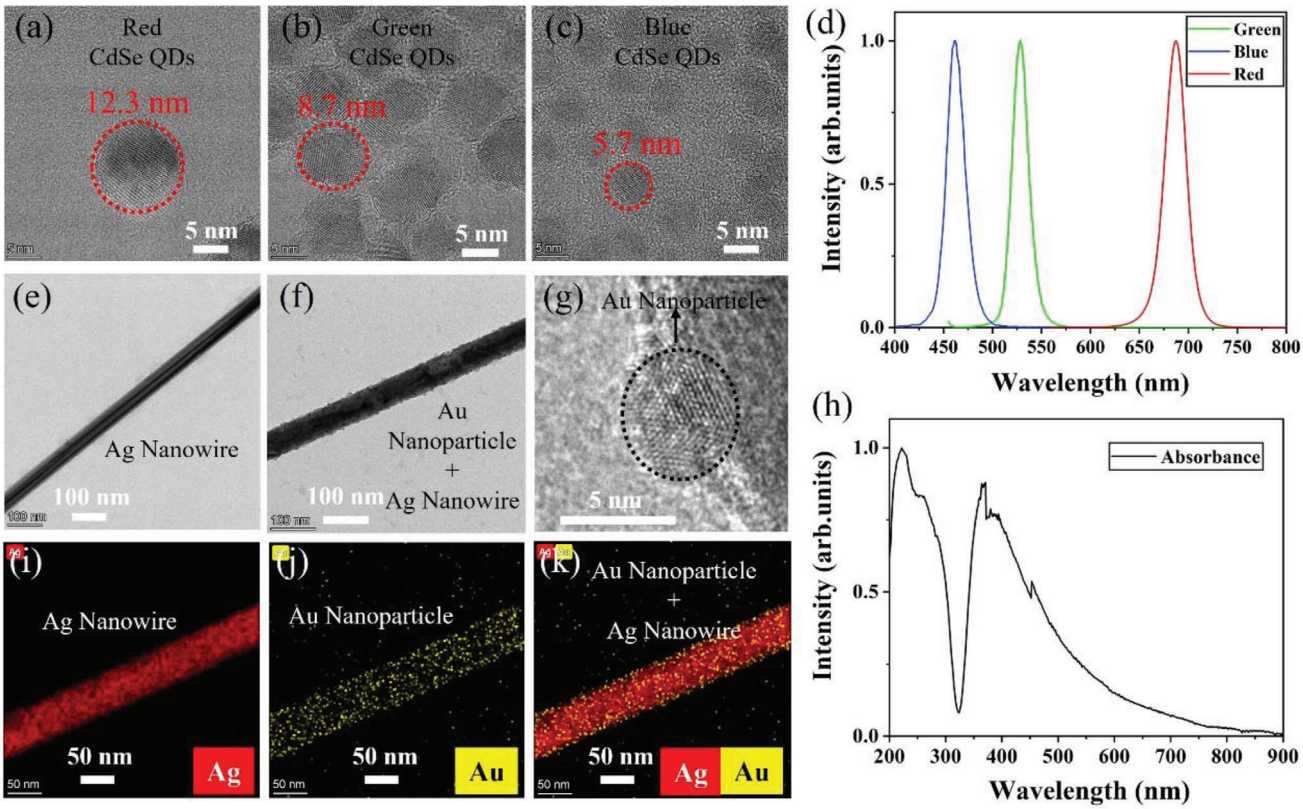

Figure 3. a–c)TEM pictures of red, green, and blue CdSe QDs. d)Normalized emission spectra of red, green, and blue CdSe QDs. e)TEM picture of Ag NWs. f) TEM picture of Au-Ag NWs. h) Normalized absorption spectrum of Au-Ag NWs. i–k)The energy dispersive X-ray spectroscopy images of the Au-Ag nanowires.

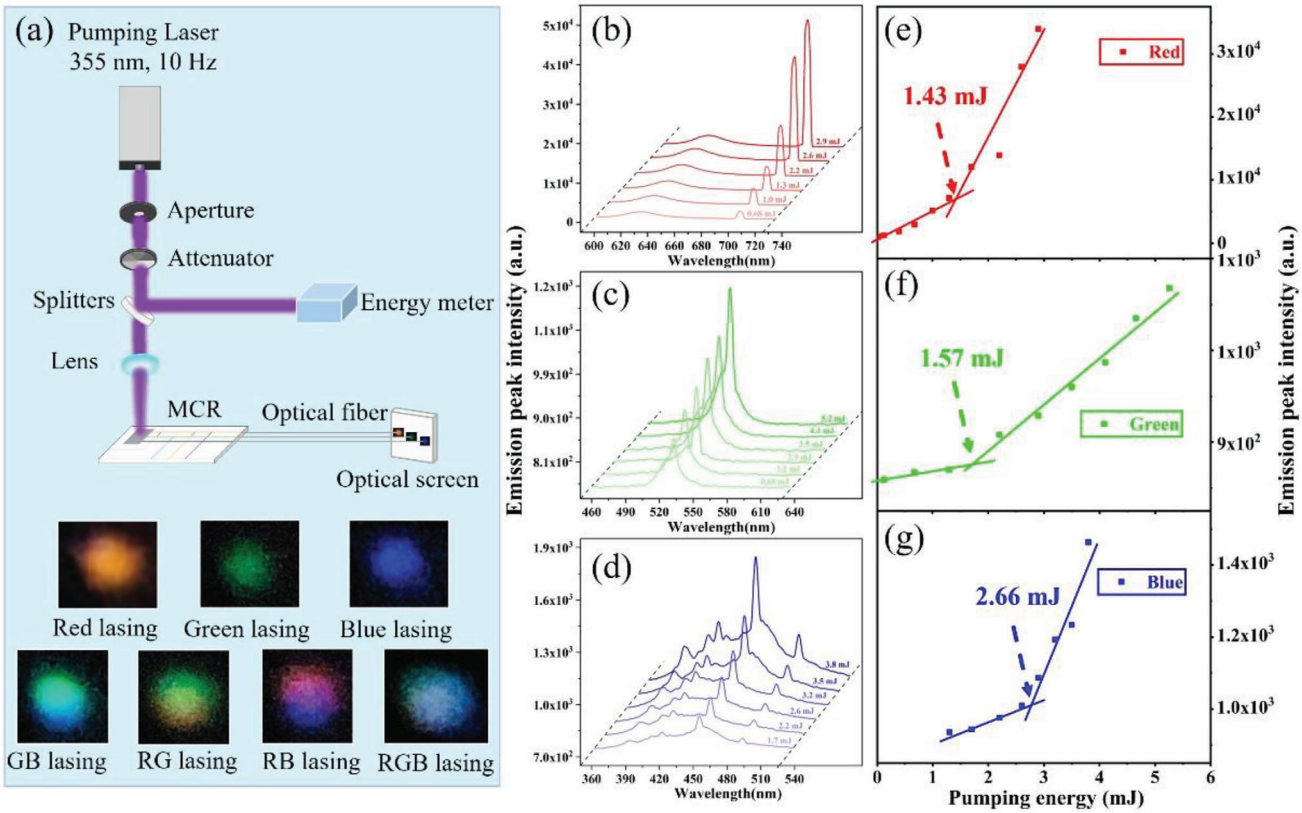

Figure 4. The lasing of the CdSe QDs and Au-Ag NWs in MCR. a) Schematic representation of the optical setup and spot images of laser output through an optical fiber. The lasing emission spectra for b) red, c) green, and d) blue from the CdSe QDs and Au-Ag NWs, pumped by 355 nm, are shown with increasing energy. Plots of the lasing emission intensity as a function of pumping energy are illustrated for e) red, f) green, and g) blue. After lens focusing, the size of the light spot is about 1 mm^2.

reaction with $HAuCl_4$. Using COMSOL 6.0 software, Figure 2b,c illustrates the electric field distribution at an incident light wavelength of 355 nm. Significantly, an enhanced standing wave resonance field is observed inside every hollow-core capillary, attributed to ultrahigh order modes (UOMs) oscillation unique to MCR.[24] The presence of this enhanced standing wave resonance field in every hollow-core capillary creates favorable conditions for the stimulated emission of CdSe QDs. Figure 2d–g showcases the electric field distribution near Ag NWs and Au-Ag NWs. The Ag NWs, with a diameter of 50 nm and a length of 1 μm, are accompanied by Au NPs with a diameter of 6 nm. The gap distance between Au NPs and Ag NWs is 2 nm. The dielectric constants of Ag and Au were chosen based on the Brendel-Bormann model. Comparative analysis reveals that the electric field around Au particles on the Ag NWs is enhanced by a factor of 10^2. Furthermore, the Ag NWs contribute to light scattering, synergizing with the MCR to facilitate the stimulated emission of quantum dots.

Under the advantageous conditions of MCR, the emission wavelength is controlled by tuning the composition of CdSe QDs, providing a much larger wavelength tuning range by changing the size of QDs. As depicted in **Figure** 3a–c, we characterized CdSe QDs to determine their chemical structure. Transmission electron microscopy (TEM) confirmed the existence of monodisperse CdSe QDs in an ethanol solution. Due to the quantum limiting effect, the emission wavelength shifted toward the blue with the decrease in quantum dot size. The emission spectra of red, green, and blue CdSe QDs under a 355 nm pump laser are depicted in Figure 3d. Figure 3e presents the TEM image of Ag NWs with an average length of ≈1 μm and a diameter of ≈50 nm. Figure 3f displays the TEM image of Au-Ag NWs, revealing numerous nano-gaps on the surface of Au-Ag NWs. Au NPs are attached to the surface of Ag NWs, forming bulges. Figure 3i–k illustrates the element distribution of Au-Ag NWs, with uniformly attached Au NPs on the surface of Ag NWs. Figure 3h presents the ultraviolet-visible absorption spectrum of Au-Ag NWs, exhibiting continuous changes in the absorption spectrum throughout the entire visible band (380 nm-780 nm). This spectrum continuously amplifies the stimulated emission process of electrons in CdSe QDs, facilitating the transition from excited state transitions to the ground state. The lasing threshold is a significant factor in laser production, and it will be addressed in the following section.

The experimental optical setup is illustrated in **Figure** 4a. Under pumping irradiation, the lasing beam passes through an aperture and an attenuator before being focused on the MCR via a lens. Utilizing free-space coupling technology, the pumping light is efficiently introduced into the MCR. Laser generation by stimulated emission occurs within the MCR, resulting in radial output along the capillary. The lasing mode in the integrated multicolor laser comes from the resonance between the UOMs in MCR and the fluorescence spectrum of CdSe quantum dots. Due to the structural limitation of MCR, the longitudinal mode

will be reflected and absorbed by the Ag film, so the final output lasing mode is the result of superposition of multiple transverse modes. The captured image of the lasing spot from the experiment is shown in Figure 4a. The experiment employs a spectrometer (Andor Shamrock 500i, Oxford Instruments) with a resolution of 0.01 nm to record the spectra of red, green, and blue lasers emitted from the MCR under different pumping energies, as depicted in Figure 4b–d. Figure 4e–g reveals the evident nonlinear change in emission intensity with increasing pumping energy. The threshold values for red, green, and blue lasers are observed at 1.43, 1.57, and 2.66 mJ, respectively. Thus, the multicolor lasing beam is simultaneously emitted under >2.66 mJ of pump light irradiation.

3. Conclusion

In summary, our proposed 2D-constrained semiconductor quantum dot integrated micro-laser, comprising a multichannel MCR and Au-Ag NWs, achieves multicolor directional output and low-threshold CdSe QDs lasing. The Au-Ag NWs contribute to multiple scattering feedback and local plasmon resonance enhancement. The MCR provides a high density of power oscillating field, enhancing the interaction between CdSe QDs and pump light and facilitating stimulated emission at a low threshold. By controlling the number of channels in which the MCR is excited, we can individually or simultaneously output red, green, blue, cyan, yellow, purple, and white lasers. This multicolor-integrated micro-laser supports the realization of active photonic chips.

Acknowledgements

M.Z. and H.D. contributed equally to this work. This research was supported by the National Key Research and Development Program of China (Grant Nos. 2017YFA0303701 and 2018YFA0306301); the National Natural Science Foundation of China (NSFC) (Grant Nos. 12104298, 11734011, 11764020, and 11974245); the Shanghai Municipal Science and Technology Major Project (Grant No. 2019SHZDZX01-06); and the Natural Science Foundation of Shanghai (23ZR1428400).

Conflict of Interest

The authors declare no conflict of interest.

Data Availability Statement

The data that support the findings of this study are available from the corresponding author upon reasonable request.

Keywords

2D constrained resonators, CdSe quantum dots, metal nanowires, multicolor lasers

Received: January 2, 2024
Revised: February 26, 2024
Published online:

[1] M. H. Huang, S. Mao, H. Feick, H. Q. Yan, Y. Y. Wu, H. Kind, E. Weber, R. Russo, P. D. Yang, *Science* **2001**, *292*, 1897.
[2] X. F. Duan, Y. Huang, R. Agarwal, C. M. Lieber, *Nature* **2003**, *421*, 241.
[3] H. Y. Liu, T. Wang, Q. Jiang, R. Hogg, F. Tutu, F. Pozzi, A. Seeds, *Nat. Photonics* **2011**, *5*, 416.
[4] R. X. Yan, D. Gargas, P. D. Yang, *Nat. Photonics* **2009**, *3*, 569.
[5] S. M. Chen, W. Li, J. Wu, Q. Jiang, M. C. Tang, S. Shutts, S. N. Elliott, A. Sobiesierski, A. J. Seeds, I. Ross, P. M. Smowton, H. Y. Liu, *Nat. Photonics* **2016**, *10*, 307.
[6] L. J. Zhang, J. W. Luo, A. Zunger, N. Akopian, V. Zwiller, J. C. Harmand, *Nano Lett.* **2010**, *10*, 4055.
[7] Q. Gao, D. Saxena, F. Wang, L. Fu, S. Mokkapati, Y. A. Guo, L. Li, J. Wong-Leung, P. Caroff, H. H. Tan, C. Jagadish, *Nano Lett.* **2014**, *14*, 5206.
[8] C. Dang, J. Lee, C. Breen, J. S. Steckel, S. Coe-Sullivan, A. Nurmikko, *Nat. Nanotechnol.* **2012**, *7*, 335.
[9] B. Piccione, C. H. Cho, L. K. van Vugt, R. Agarwal, *Nat. Nanotechnol.* **2012**, *7*, 640.
[10] J. Y. Xu, X. J. Zhuang, P. F. Guo, Q. L. Zhang, W. Q. Huang, Q. Wan, W. Hu, X. X. Wang, X. L. Zhu, C. Z. Fan, Z. Y. Yang, L. M. Tong, X. F. Duan, A. L. Pan, *Nano Lett.* **2012**, *12*, 5003.
[11] C. Zhang, L. Yang, J. Zhao, B. H. Liu, M. Y. Han, Z. P. Zhang, *Angew. Chem.* **2015**, *127*, 11693.
[12] U. Demirbas, *J. Opt. Soc. Am. B* **2018**, *35*, 2994.
[13] P. K. Roy, G. Haider, H. I. Lin, Y. M. Liao, C. H. Lu, K. H. Chen, L. C. Chen, W. H. Shih, C. T. Liang, Y. F. Chen, *Adv. Opt. Mater.* **2018**, *6*, 1800382.
[14] X. T. Jiang, X. M. Zhao, W. L. Bao, R. C. Shi, J. L. Zhao, J. L. Kang, X. F. Xia, H. L. Chen, H. B. Li, J. L. Xu, H. Zhang, *ACS Appl. Nano Mater.* **2020**, *3*, 4990.
[15] Y. Feng, S. H. Huang, A. Shirakawa, K. Ueda, *Opt. Express* **2004**, *12*, 1843.
[16] S. Yakunin, L. Protesescu, F. Krieg, M. I. Bodnarchuk, G. Nedelcu, M. Humer, G. De Luca, M. Fiebig, W. Heiss, M. V. Kovalenko, *Nat. Commun.* **2015**, *6*, 8056.
[17] C. H. Zhang, C. L. Zou, H. Y. Dong, Y. L. Yan, J. N. Yao, Y. S. Zhao, *Sci. Adv.* **2017**, *3*, e1700225.
[18] Q. Zhang, Q. Y. Shang, J. Shi, J. Chen, R. Wang, Y. Mi, W. N. Du, C. Shen, R. M. Ma, X. H. Qiu, X. F. Liu, T. C. Sum, *ACS Photonics* **2017**, *4*, 2789.
[19] Q. Zhang, R. Su, X. F. Liu, J. Xing, T. C. Sum, Q. H. Xiong, *Adv. Funct. Mater.* **2016**, *26*, 6238.
[20] H. M. Zhu, Y. P. Fu, F. Meng, X. X. Wu, Z. Z. Gong, Q. Ding, M. V. Gustafsson, M. T. Trinh, S. Jin, X. Y. Zhu, *Nat. Mater.* **2015**, *14*, 636.
[21] Y. S. Park, J. Roh, B. T. Diroll, R. D. Schaller, V. I. Klimov, *Nat. Rev. Mater.* **2021**, *6*, 382.
[22] H. L. Dai, C. Yin, Z. Y. Xiao, Z. Q. Cao, X. F. Chen, *Phys. Rev. Appl.* **2019**, *11*, 064055.
[23] H. G. Li, Z. Q. Cao, H. F. Lu, Q. S. Shen, *Appl. Phys. Lett.* **2003**, *83*, 2757.
[24] H. Yang, H. L. Dai, Q. H. Wei, H. R. Shan, Z. Q. Cao, X. F. Chen, *Phys. Rev. Appl.* **2021**, *16*, 034015.